Lithium Diisopropylamide-Mediated Enolization:

Catalysis by Hemilabile Ligands

Antonio Ramírez, Xiufeng Sun, David B. Collum*

Contribution from the Department of Chemistry and Chemical Biology

Baker Laboratory, Cornell University

Ithaca, New York 14853-1301

Supporting Information

		Page
Part 1: Experimental Procedures		S3
Part 2: NMR Spectroscopic Studies		
I	^{6}Li and ^{15}N NMR spectra of [^{6}Li,^{15}N]LDA with **7** in *n*-BuOMe	S4
II	^{6}Li and ^{15}N NMR spectra of [^{6}Li,^{15}N]LDA with **7** in amino ether **B**	S5
III	^{6}Li and ^{15}N NMR spectra of [^{6}Li,^{15}N]LDA with **7** in amino ether **C**	S7
IV	^{6}Li and ^{15}N NMR spectra for the enolization of **1** in *n*-BuOMe	S8
V	^{6}Li and ^{15}N NMR spectra for the enolization of **1** in amino ether **B**	S9
VI	^{6}Li and ^{15}N NMR spectra for the enolization of **1** in amino ether **C**	S10
VII	^{6}Li NMR spectra of ester enolates **14**	S11
VIII	^{13}C NMR spectra of mixed dimer $\mathbf{12_B}$ in the slow solvent exchange limit	S12
Part 3: Rate Studies		
IX	Plot of k_{obsd} vs [*n*-BuOMe] for the enolization of **7**	S13
X	Plot of k_{obsd} vs [LDA] for the enolization of **7** in *n*-BuOMe	S14
XI	Plot of k_{obsd} vs [**B**] for the enolization of **7**	S15
XII	Plot of k_{obsd} vs [LDA] for the enolization of **7** in amino ether **B**	S16

XIII Plot of k_{obsd} vs [**C**] for the enolization of **7** S17

XIV Plot of k_{obsd} vs [LDA] for the enolization of **7** in amino ether **C** S18

XV Plot of k_{obsd} vs [**B**] for the enolization of **2** by mixed dimer $\mathbf{12_B}$ S19

XVI Plot of k_{obsd} vs [$\mathbf{14_B}$] for the enolization of **2** by mixed dimer $\mathbf{12_B}$ S20

XVII Plot of k_{obsd} vs [$\mathbf{12_B}$] for the enolization of **2** by mixed dimer $\mathbf{12_B}$ S21

XVIII Representative enolization of **2** by 1.0 equiv of LDA S22

XIX Representative enolization of **2** catalyzed by amino ether **B** S22

Part 4: DFT Computational Studies

XX Geometries and *G*'s of miscellaneous aggregates S23

XXI Geometries and *G*'s of miscellaneous chelated aggregates S25

XXII Selected bond lengths and angles of aggregates in Section **XXI** S27

XXIII Geometries and *G*'s of monomer- and dimer-based transition structures S29

XXIV Geometries and *G*'s of mixed aggregate-based transition structures S30

XXV Selected bond lengths and angles of TS's in Sections **XXIII** and **XXIV** S31

Part 5: References S32

Part 1: Experimental Procedures

Lithiated Enolate 2. A flame dried 250 mL round bottom flask was charged with recrystallized LDA[S-1] (3.0 g, 28 mmol) and 60 mL of freshly distilled hexanes under argon. After heating to dissolve the LDA and cooling to 0 °C, ester **2** (5.5 mL, 30 mmol) was added slowly. Stirring at room temperature for 10 h followed by partial evaporation of hexanes under vacuum and cooling to 0 °C led to significant formation of a white solid. Further precipitation was achieved by cooling the reaction mixture to -78 ºC for 0.5 h. Filtration, washing with 5 x 10 mL fresh hexanes, and drying in vacuo yielded 2.2 g of enolate **3** (11.8 mmol, 86 %) as a white powder that was stored in a dry box.

Ligands **B** and **C** were prepared following described procedures. Ligand **B**: Remenar, J. F.; Lucht, B. L.; Collum, D. B. *J. Am. Chem. Soc.* **1997**, *119*, 5567. Ligand **C**: Brown, H. C.; Zaidlewicz, M.; Dalvi, P. V.; Narasimhan, S.; Mukhopadyay, A. *Organometallics* **1999**, *18*, 1305.

Ester **2** and carboxamide **7** were prepared following described procedures. Ester **2**: Ohta, S.; Shimabayashi, A.; Aono, M.; Okamoto, M. *Synthesis* **1982**, *10*, 833. Carboxamide **7**: Matsuda, F.; Itoh, S.; Hattori, N.; Yanagiya, M.; Matsumoto, T. *Tetrahedron* **1985**, *41*, 3625.

Part 2: NMR Spectroscopic Studies

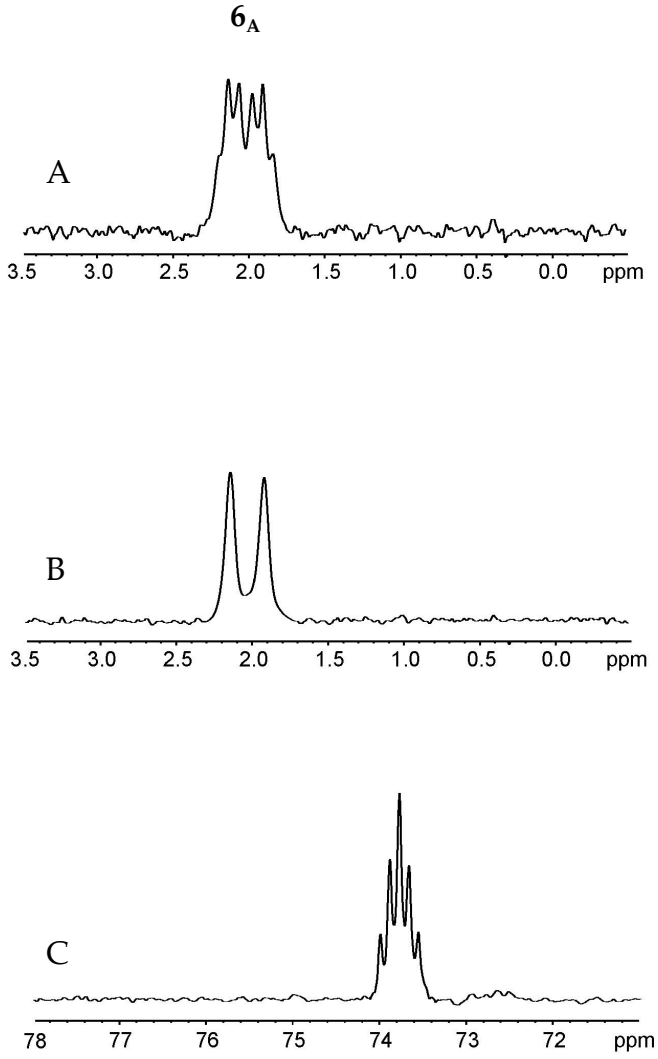

I. ^{6}Li and ^{15}N NMR spectra of 0.10 M [^{6}Li,^{15}N]LDA with 0.5 equiv carboxamide **7** and 1.0 M *n*-BuOMe (**A**) in cyclopentane at –125 ^{o} C. (A) ^{6}Li spectrum; (B) ^{6}Li{^{15}N} spectrum; (C) ^{15}N spectrum.

6_B

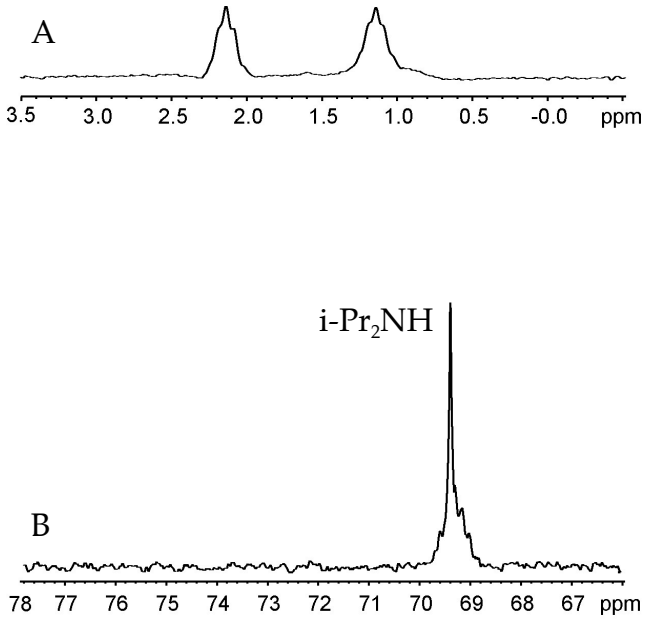

II. ^{6}Li and ^{15}N NMR spectra of 0.10 M [^{6}Li,^{15}N]LDA with 0.5 equiv carboxamide **7** and 1.0 M $MeOCH_2CH_2NMe_2$ (**B**) in cyclopentane at –125 ^{o} C. (A) ^{6}Li spectrum; (B) ^{15}N spectrum.

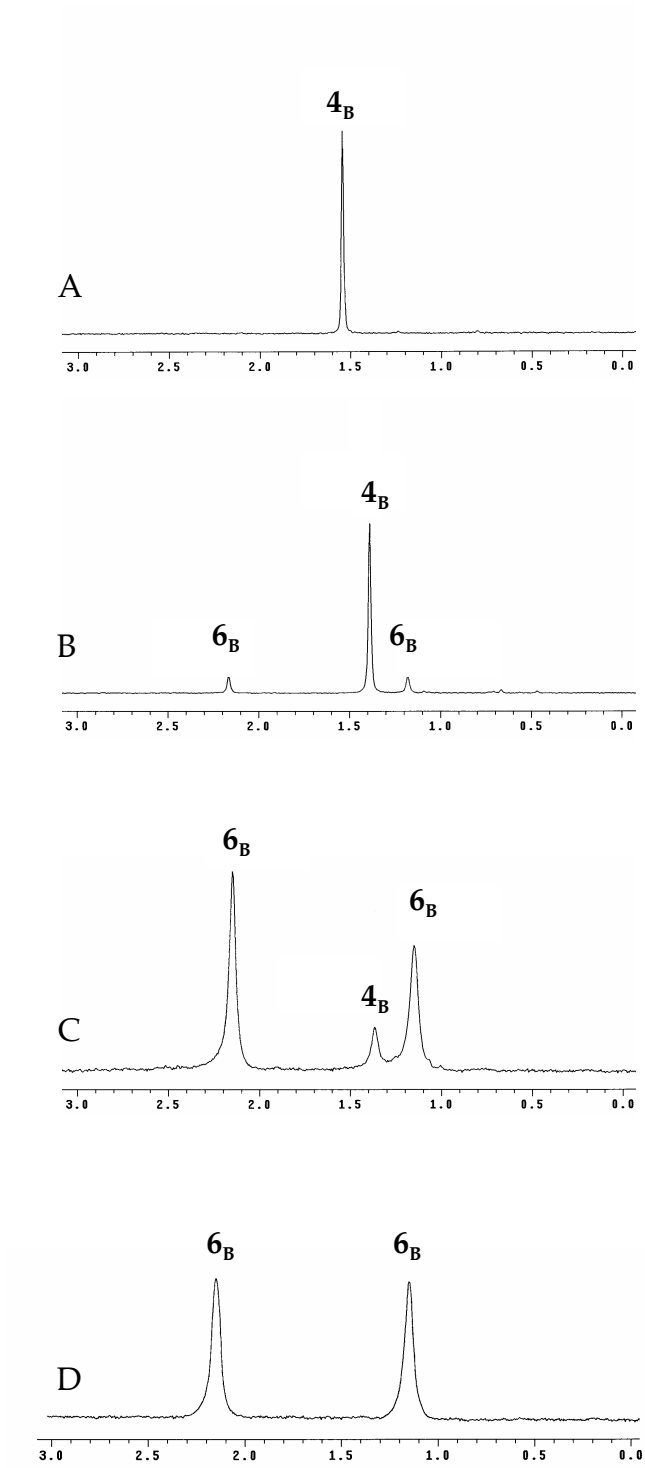

II (*Continued*)**.** ^{6}Li NMR spectra of 0.10 M [^{6}Li]LDA with carboxamide **7** and 1.5 M $MeOCH_2CH_2NMe_2$ (**B**) at –120 ° C. (A) ^{6}Li spectrum with no carboxamide; (B) ^{6}Li spectrum with 0.1 equiv carboxamide; (C) ^{6}Li spectrum with 0.4 equiv carboxamide; (D) ^{6}Li spectrum with 0.5 equiv carboxamide.

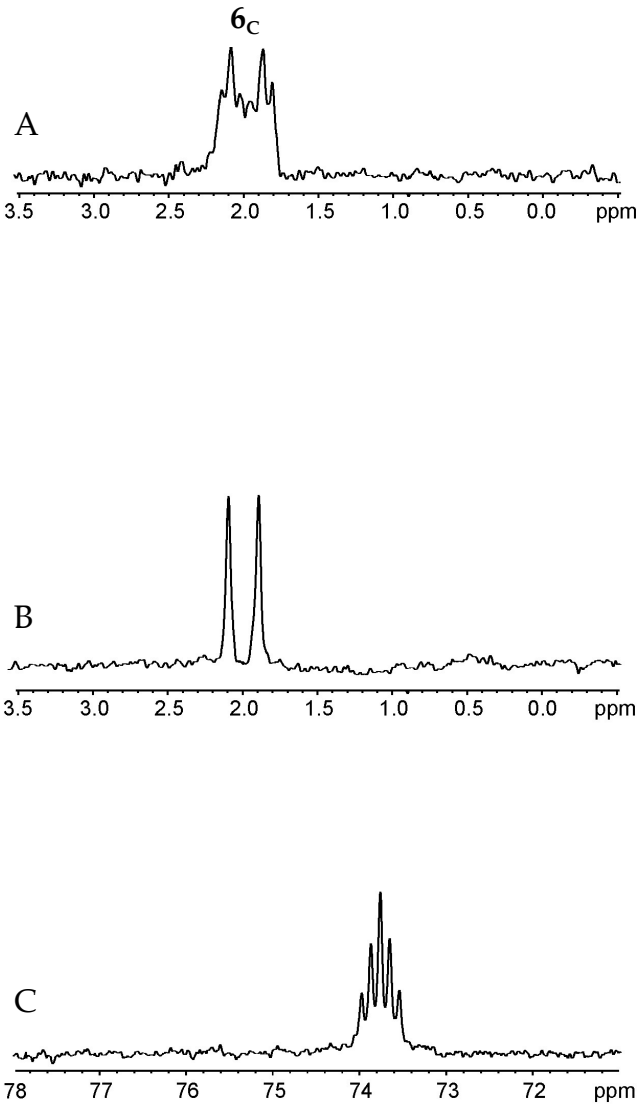

III. ^{6}Li and ^{15}N NMR spectra of 0.10 M [^{6}Li,^{15}N]LDA with 0.5 equiv carboxamide **7** and 1.0 M $MeOCH_2CH_2N(i\text{-}Pr)_2$ (**C**) in cyclopentane at –125 ^{o} C. (A) ^{6}Li spectrum; (B) ^{6}Li{^{15}N} spectrum; (C) ^{15}N spectrum.

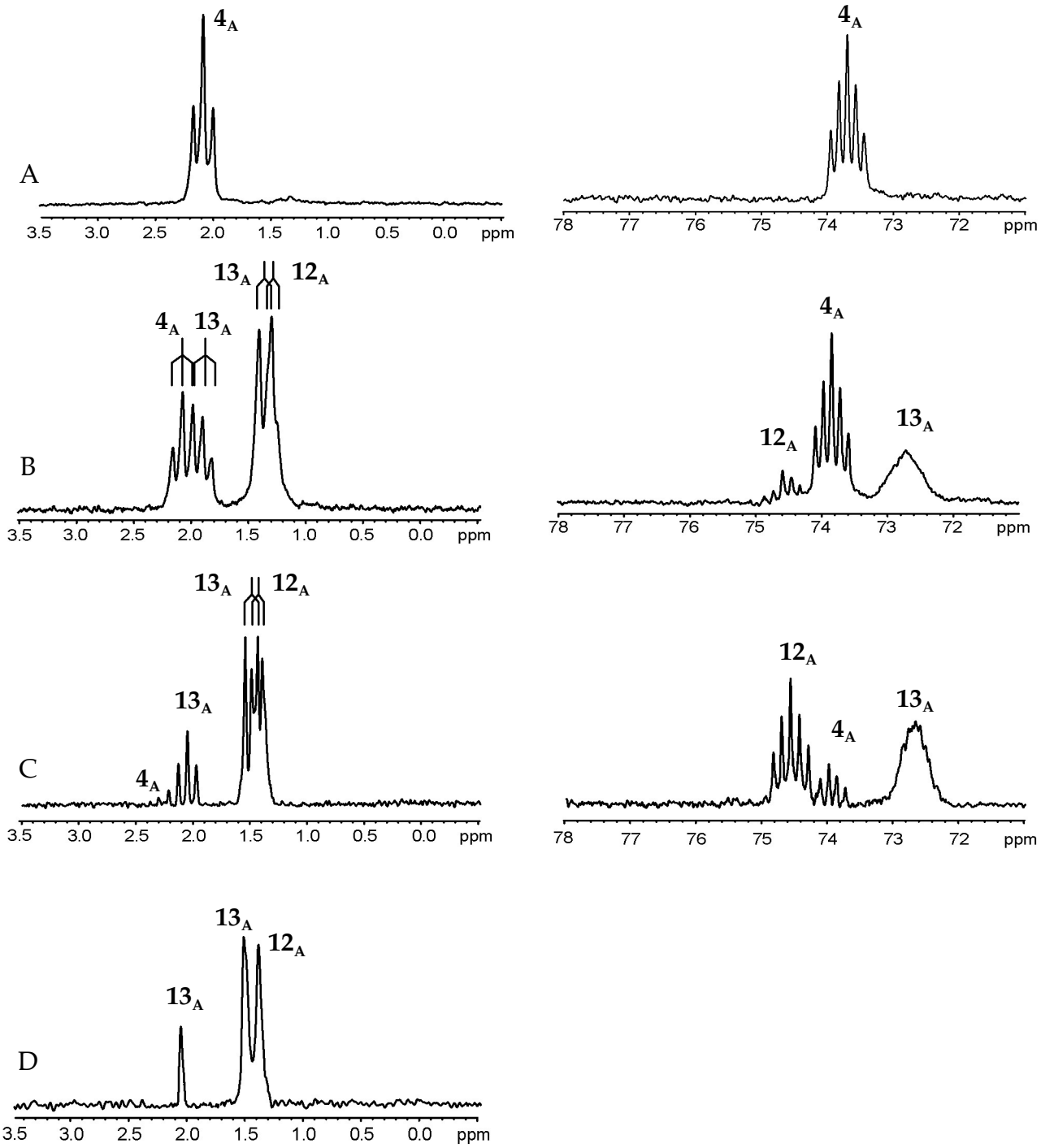

IV. ^{6}Li and ^{15}N NMR spectra of 0.10 M [^{6}Li,^{15}N]LDA with 0.10 M ester **2** and 1.0 M *n*-BuOMe (**A**) in pentane at -90 °C. (A) Spectra recorded before the sample was aged. (B) Spectra recorded after the sample was aged at 0 °C for 10 min. (C) Spectra recorded after the sample was aged at 0 °C for 30 min. (D) ^{6}Li{^{15}N} spectrum recorded on sample C.

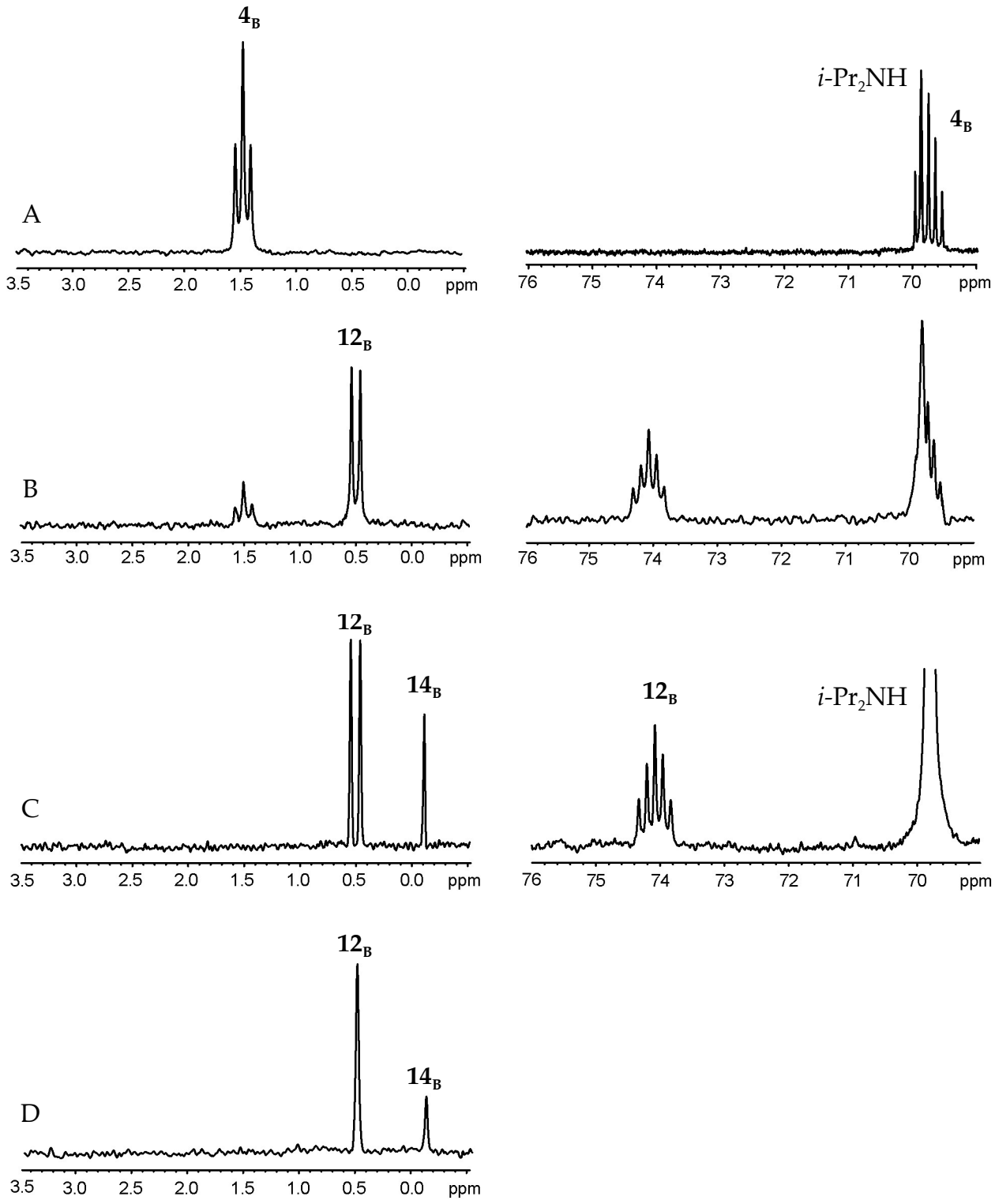

V. ^{6}Li and ^{15}N NMR spectra of (A) 0.10 M [^{6}Li,^{15}N]LDA and 1.0 M $Me_2OCH_2CH_2NMe_2$ (**B**) in pentane at -90 °C. (B) 0.10 M [^{6}Li,^{15}N]LDA with 0.10 M ester **2** and 1.0 M **B** in pentane at -90 °C: ^{6}Li and ^{15}N spectra recorded after the sample was aged at -90 °C for 45 min. (C) ^{6}Li and ^{15}N spectra recorded after the sample was aged at -90 °C for 60 min. (D) ^{6}Li{^{15}N} spectrum recorded on sample C.

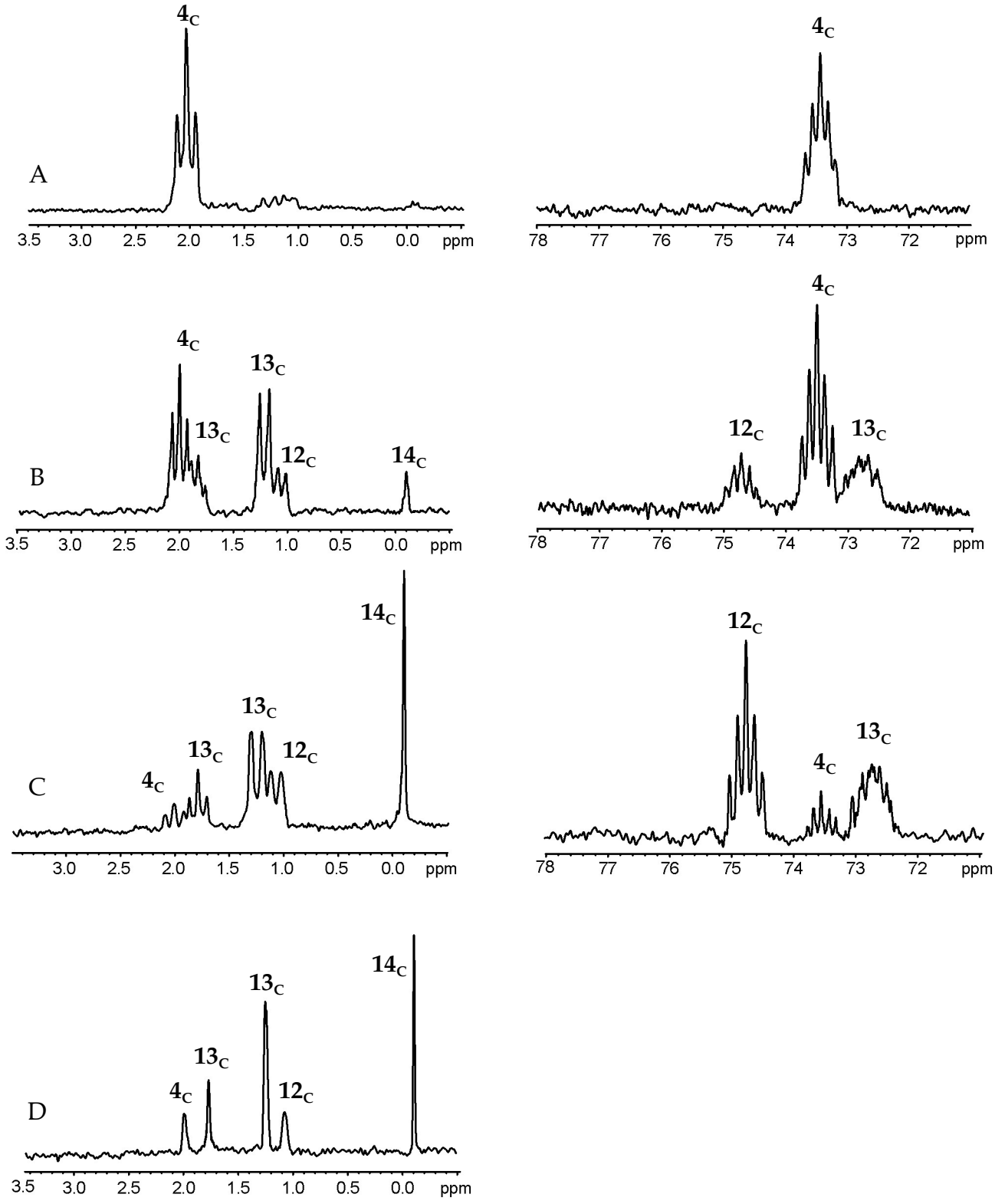

VI. ^{6}Li and ^{15}N NMR spectra of 0.10 M [^{6}Li,^{15}N]LDA with 0.10 M ester **2** and 1.0 M $MeOCH_2CH_2N(i\text{-}Pr)_2$ (**C**) in pentane at -90 °C. (A) Spectra recorded before the sample was aged. (B) ^{6}Li and ^{15}N spectra recorded after the sample was aged at 0 °C for 5 min. (C) ^{6}Li and ^{15}N spectra recorded after the sample was aged at 0 °C for 15 min. (D) ^{6}Li{^{15}N} spectrum recorded on sample C.

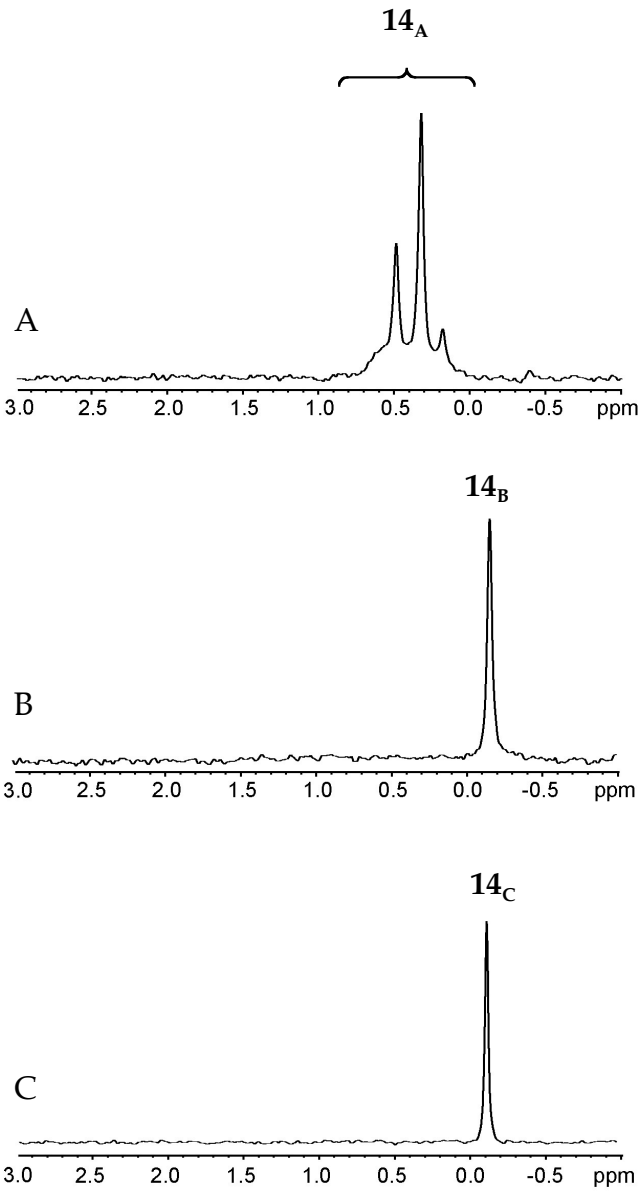

VII. ^{6}Li NMR spectra of 0.15 M ester enolates **14** at -90 °C in pentane cosolvent and (A) 1.0 M *n*-BuOMe (**A**); (B) 1.0 M $MeOCH_2CH_2NMe_2$ (**B**); (C) 1.0 M $MeOCH_2CH_2N(i\text{-}Pr)_2$ (**C**).

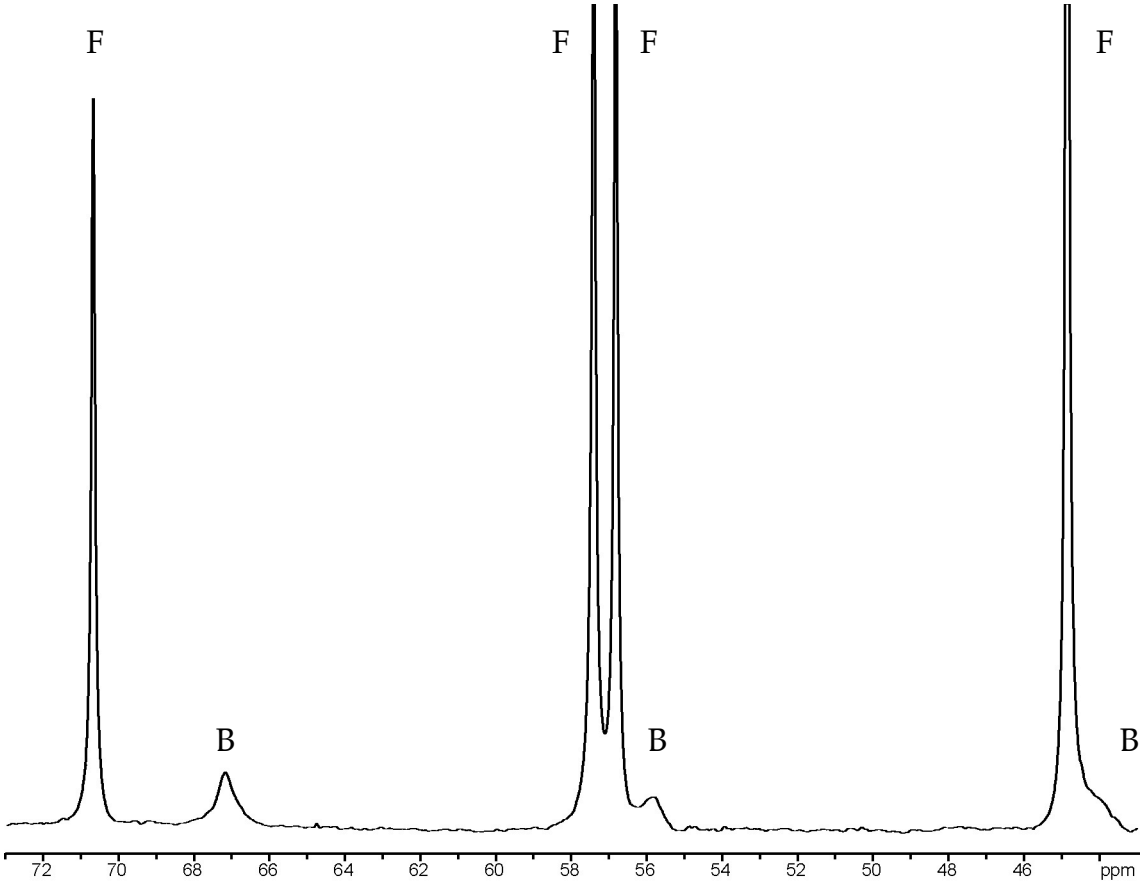

VIII. $^{13}C\{^{1}H\}$ spectrum of 0.1 M [^{6}Li]**12**$_{\mathbf{B}}$ in cyclopentane at -125 °C containing 8.0 equiv of $Me_2OCH_2CH_2NMe_2$ (**B**). Free ligand: $F^{[S-2]}$, bound ligand: B.

Part 3: Rate Studies

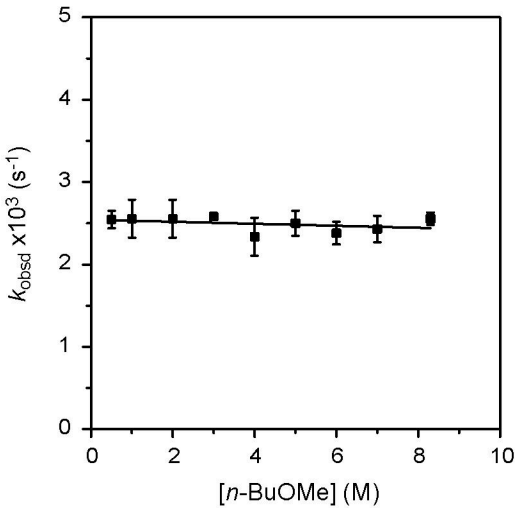

IX. Plot of k_{obsd} vs [*n*-BuOMe] (**A**) in hexane cosolvent for the enolization of **7** (0.004 M) by LDA (0.10 M) at 0 °C. The curve depicts an unweighted least-squares fit to $k_{obsd} = k$[*n*-BuOMe] + k' (k = (-1 ± 1) x 10^{-5}, k' = (2.5 ± 0.1) x 10^{-3}).

[*n*-BuOMe] (M)	k_{obsd}1 x 10^3 (s^{-1})	k_{obsd}2 x 10^3 (s^{-1})	k_{obsd}av (s^{-1})
0.5	0.0026 ± 2E-4	0.0025 ± 2E-4	0.0025 ± 1E-4
1.0	0.0027 ± 2E-4	0.0024 ± 1E-4	0.0025 ± 2E-4
2.0	0.0027 ± 2E-4	0.0024 ± 1E-4	0.0025 ± 2E-4
3.0	0.00255 ± 8E-5	0.0026 ± 2E-4	0.00258 ± 4E-5
4.0	0.0022 ± 1E-4	0.0025 ± 2E-4	0.0023 ± 2E-4
5.0	0.0024 ± 2E-4	0.0026 ± 2E-4	0.0025 ± 1E-4
6.0	0.00248 ± 7E-5	0.0023 ± 1E-4	0.0024 ± 1E-4
7.0	0.00254 ± 8E-5	0.00231 ± 8E-5	0.0024 ± 2E-4
8.3	0.0026 ± 2E-4	0.0025 ± 1E-4	0.00255 ± 8E-5

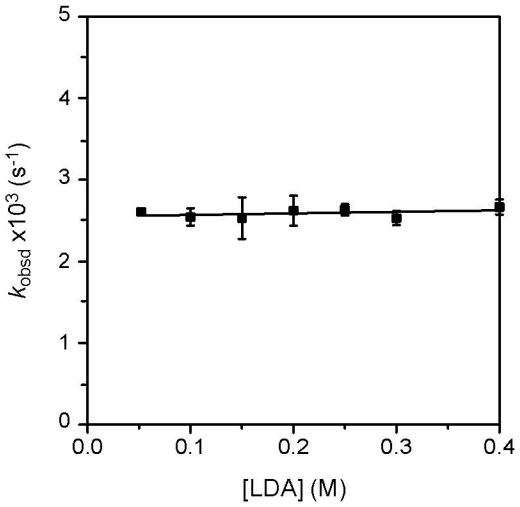

X. Plot of k_{obsd} vs [LDA] in *n*-BuOMe (**A**, 0.5 M) and hexane cosolvent for the enolization of **7** (0.004 M) at 0 °C. The curve depicts an unweighted least-squares fit to $k_{obsd} = k[\text{LDA}] + k'$ ($k = (2 \pm 2) \times 10^{-4}$, $k' = (2.5 \pm 0.1) \times 10^{-3}$).

[LDA] (M)	$k_{obsd}1 \times 10^3$ (s^{-1})	$k_{obsd}2 \times 10^3$ (s^{-1})	k_{obsd}av $\times 10^3$ (s^{-1})
0.05	0.0026 ± 1E-4	0.0026 ± 2E-4	0.0026 ± 1E-4
0.10	0.0026 ± 2E-4	0.0025 ± 2E-4	0.0025 ± 1E-4
0.15	0.0023 ± 1E-4	0.0027 ± 1E-4	0.0025 ± 2E-4
0.20	0.0027 ± 2E-4	0.00249 ± 6E-5	0.0026 ± 2E-4
0.25	0.0026 ± 2E-4	0.00268 ± 8E-5	0.0026 ± 1E-4
0.30	0.0026 ± 1E-4	0.0025 ± 1E-4	0.0025 ± 1E-4
0.40	0.0026 ± 1E-4	0.0027 ± 2E-4	0.0027 ± 1E-4

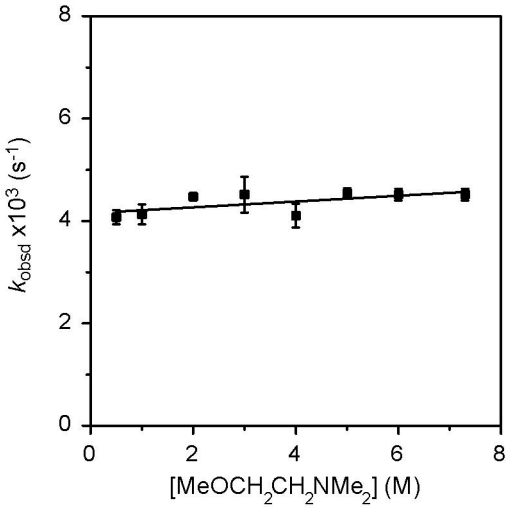

XI. Plot of k_{obsd} vs [$MeOCH_2CH_2NMe_2$] (**B**) in hexane cosolvent for the enolization of **7** (0.004 M) by LDA (0.10 M) at -40 °C. The curve depicts an unweighted least-squares fit to $k_{obsd} = k[MeOCH_2CH_2NMe_2] + k'$ ($k = (6 \pm 3) \times 10^{-5}$, $k' = (4.1 \pm 0.1) \times 10^{-3}$).

[**3**] (M)	$k_{obsd}1 \times 10^3$ (s^{-1})	$k_{obsd}2 \times 10^3$ (s^{-1})	$k_{obsd}av \times 10^3$ (s^{-1})
0.5	0.0042 ± 1E-4	0.00397 ± 8E-5	0.0041 ± 1E-4
1.0	0.00399 ± 9E-5	0.0043 ± 2E-4	0.0041 ± 2E-4
2.0	0.0044 ± 2E-4	0.00451 ± 9E-5	0.00448 ± 6E-5
3.0	0.0043 ± 2E-4	0.0048 ± 2E-4	0.0045 ± 3E-4
4.0	0.0039 ± 2E-4	0.0043 ± 2E-4	0.0041 ± 2E-4
5.0	0.0045 ± 1E-4	0.00461 ± 8E-5	0.0045 ± 1E-5
6.0	0.00443 ± 9E-5	0.0046 ± 3E-4	0.0045 ± 1E-4
7.3	0.0044 ± 1E-4	0.0046 ± 2E-4	0.0045 ± 1E-4

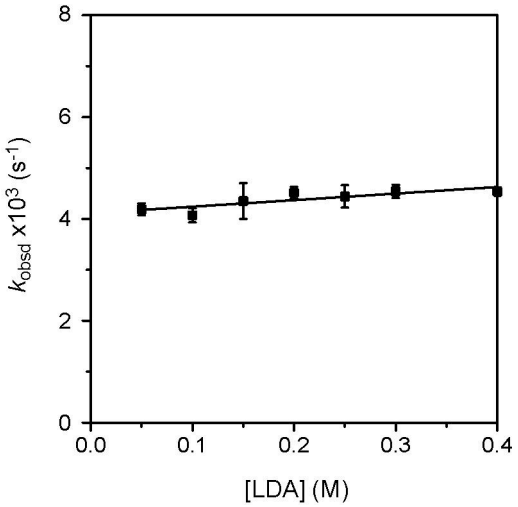

XII. Plot of k_{obsd} vs [LDA] in $MeOCH_2CH_2NMe_2$ (**B**, 0.5 M) and hexane cosolvent for the enolization of **7** (0.004 M) at -40 °C. The curve depicts an unweighted least-squares fit to $k_{obsd} = k[LDA] + k'$ ($k = (1.2 \pm 0.3) \times 10^{-3}$, $k' = (4.1 \pm 0.1) \times 10^{-3}$).

[LDA] (M)	$k_{obsd}1 \times 10^3$ (s^{-1})	$k_{obsd}2 \times 10^3$ (s^{-1})	$k_{obsd}av \times 10^3$ (s^{-1})
0.05	0.0041 ± 2E-4	0.0043 ± 2E-4	0.0042 ± 1E-4
0.10	0.0042 ± 1E-4	0.00397 ± 8E-5	0.0041 ± 1E-4
0.15	0.0041 ± 2E-4	0.0046 ± 2E-4	0.0043 ± 3E-4
0.20	0.0046 ± 2E-4	0.0044 ± 2E-4	0.0045 ± 1E-4
0.25	0.00428 ± 9E-5	0.0046 ± 2E-4	0.0044 ± 2E-4
0.30	0.00463 ± 8E-5	0.00445 ± 9E-5	0.0045 ± 1E-5
0.40	0.00448 ± 8E-5	0.0046 ± 2E-4	0.00454 ± 8E-5

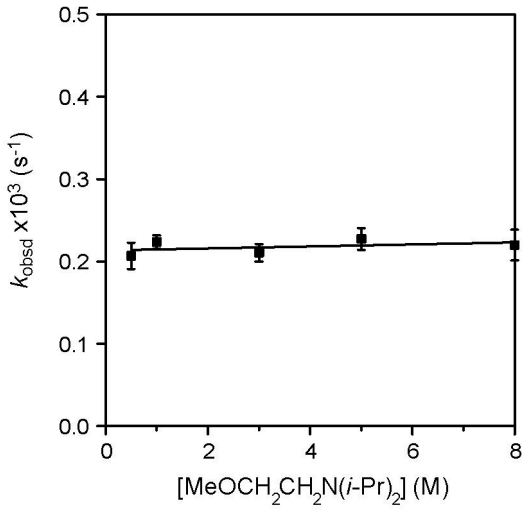

XIII. Plot of k_{obsd} vs [MeOCH$_2$CH$_2$N(*i*-Pr)$_2$] (**C**) in hexane cosolvent for the enolization of **7** (0.004 M) by LDA (0.10 M) at -30 °C. The curve depicts an unweighted least-squares fit to $k_{obsd} = k$[MeOCH$_2$CH$_2$N(*i*-Pr)$_2$] + k' (k =(1 $\pm$ 1) x 10^{-6}, k' = (2.1 $\pm$ 0.1) x 10^{-4}).

[**C**] (M)	k_{obsd}1 x 10^3 (s^{-1})	k_{obsd}2 x 10^3 (s^{-1})	k_{obsd}av x 10^3 (s^{-1})
0.5	0.00022 $\pm$ 2E-5	0.00019 $\pm$ 2E-5	0.00021 $\pm$ 2E-5
1.0	0.00023 $\pm$ 3E-5	0.00022 $\pm$ 3E-5	0.00022 $\pm$ 1E-5
3.0	0.00020 $\pm$ 2E-5	0.00022 $\pm$ 3E-5	0.00021 $\pm$ 1E-5
5.0	0.00024 $\pm$ 2E-5	0.00022 $\pm$ 2E-5	0.00023 $\pm$ 1E-5
8.0	0.00021 $\pm$ 3E-5	0.00023 $\pm$ 2E-5	0.00022 $\pm$ 2E-5

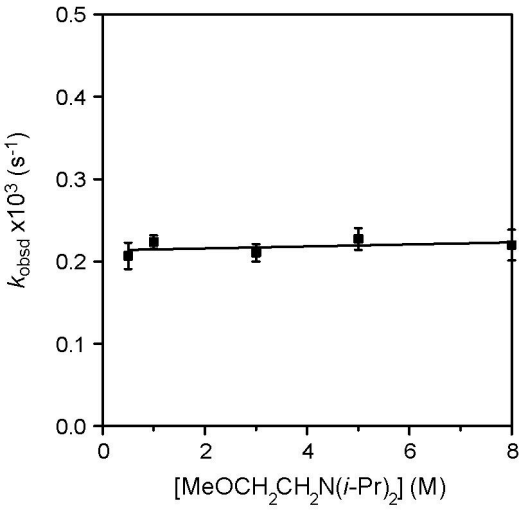

XIV. Plot of k_{obsd} vs [LDA] in MeOCH$_2$CH$_2$N(*i*-Pr)$_2$ (**C**, 0.5 M) and hexane cosolvent for the enolization of **7** (0.004 M) at -30 °C. The curve depicts an unweighted least-squares fit to $k_{obsd} = k$[LDA] + k' (k = (1.0 ± 0.3) x 10^{-4}, k' = (2.0 ± 0.6) x 10^{-4}).

[LDA] (M)	$k_{obsd}1$ x 10^3 (s^{-1})	$k_{obsd}2$ x 10^3 (s^{-1})	k_{obsd}av x 10^3 (s^{-1})
0.05	0.00020 ± 2E-5	0.00023 ± 2E-5	0.00021 ± 2E-5
0.10	0.00022 ± 2E-5	0.00019 ± 2E-5	0.00021 ± 2E-5
0.20	0.00023 ± 3E-5	0.00023 ± 2E-5	0.00023 ± 1E-5
0.30	0.00022 ± 2E-5	0.00024 ± 3E-5	0.00023 ± 1E-5
0.40	0.00026 ± 3E-5	0.00023 ± 2E-5	0.00025 ± 2E-5

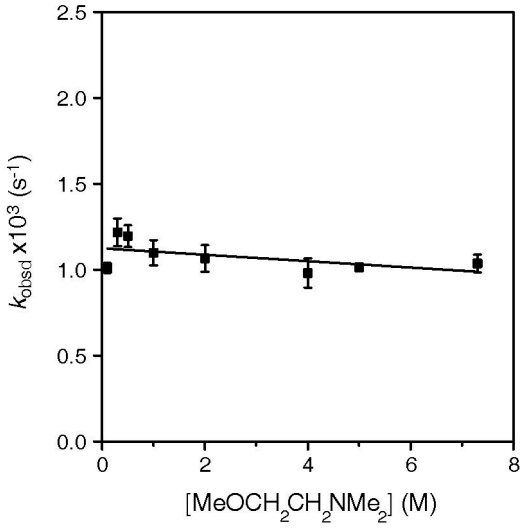

XV. Plot of k_{obsd} vs [$MeOCH_2CH_2NMe_2$] (**B**) in hexane cosolvent for the enolization of ester **2** (0.002 M) by mixed dimer $\mathbf{12_B}$ (0.05 M) at -60 °C in the presence of excess enolate $\mathbf{14_B}$ (0.005 M). The curve depicts an unweighted least-squares fit to $k_{obsd} = k[MeOCH_2CH_2NMe_2] + k'$ ($k = (-1 \pm 1) \times 10^{-5}$, $k' = (1.1 \pm 0.1) \times 10^{-3}$).

[**3**] (M)	$k_{obsd}1 \times 10^3$ (s^{-1})	$k_{obsd}2 \times 10^3$ (s^{-1})	k_{obsd}av $\times 10^3$ (s^{-1})
0.1	0.99 ± 5E-2	1.03 ± 8E-2	1.01 ± 3E-2
0.3	1.27 ± 7E-2	1.16 ± 3E-2	1.21 ± 8E-2
0.5	1.24 ± 7E-2	1.15 ± 3E-2	1.19 ± 6E-2
1.0	1.05 ± 8E-2	1.15 ± 7E-2	1.10 ± 7E-2
2.0	1.01 ± 5E-2	1.12 ± 4E-2	1.06 ± 8E-2
4.0	1.04 ± 5E-2	0.92 ± 3E-2	0.98 ± 8E-2
5.0	9.98 ± 7E-2	1.03 ± 8E-2	1.01 ± 2E-2
7.3	1.00 ± 6E-2	1.1 ± 1E-1	1.04 ± 5E-2

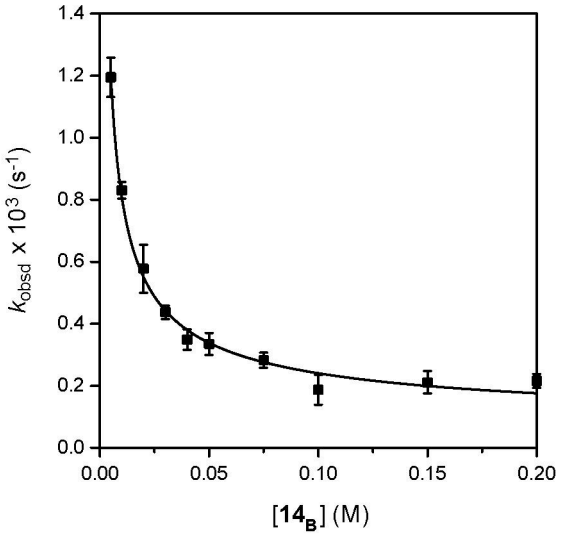

XVI. Plot of k_{obsd} vs enolate [$\mathbf{14_B}$] in hexane cosolvent for the enolization of ester **2** (0.002 M) by mixed dimer $\mathbf{12_B}$ (0.05 M) at -60 °C. The curve depicts an un-weighted least-squares fit to $k_{obsd} = k[\mathbf{14_B}]^n \pm k'$ (k = (5 ± 2) x 10^{-5}, n = -0.61 ± 0.07, k' = (5 ± 5) x 10^{-5}).

[$\mathbf{14_B}$] (M)	$k_{obsd}1$ x 10^3 (s^{-1})	$k_{obsd}2$ x 10^3 (s^{-1})	k_{obsd}av x 10^3 (s^{-1})
0.005	1.24 ± 7E-2	1.15 ± 3E-2	1.19 ± 6E-2
0.010	0.81 ± 7E-2	0.85 ± 9E-2	0.83 ± 3E-2
0.020	0.52 ± 3E-2	0.63 ± 3E-2	0.58 ± 8E-2
0.030	0.45 ± 4E-2	0.42 ± 2E-2	0.44 ± 2E-2
0.040	0.37 ± 3E-2	0.32 ± 1E-2	0.35 ± 3E-2
0.050	0.36 ± 3E-2	0.31 ± 2E-2	0.33 ± 3E-2
0.075	0.30 ± 3E-2	0.26 ± 3E-2	0.28 ± 2E-2
0.10	0.15 ± 1E-2	0.22 ± 1E-2	0.19 ± 5E-2
0.15	0.24 ± 1E-2	0.18 ± 2E-2	0.21 ± 4E-2
0.20	0.20 ± 2E-2	0.23 ± 2E-2	0.21 ± 2E-2

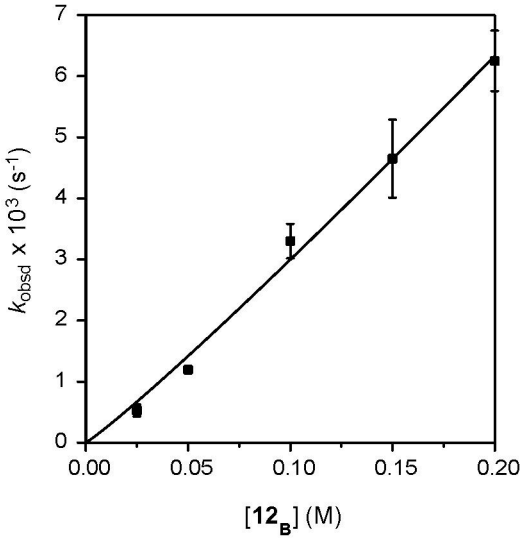

XVII. Plot of k_{obsd} vs mixed dimer [$\mathbf{12_B}$] in hexane cosolvent for the enolization of ester **2** (0.002 M) at -60 °C in the presence of excess enolate $\mathbf{14_B}$ (0.005 M). The curve depicts an unweighted least-squares fit to $k_{obsd} = k[\mathbf{12_B}]^n + k'$ (k = (3.4 ± 0.6) x 10^{-2}, n = 1.0 + 0.1, k' = (1 ± 2) x 10^{-4}).

[$\mathbf{12_B}$] (M)	k_{obsd}1 x 10^3 (s^{-1})	k_{obsd}2 x 10^3 (s^{-1})	k_{obsd}av x 10^3 (s^{-1})
0.025	0.59 ± 4E-2	0.46 ± 6E-2	0.53 ± 9E-2
0.050	1.24 ± 7E-2	1.15 ± 3E-2	1.19 ± 6E-2
0.10	3.5 ± 3E-1	3.11 ± 8E-2	3.3 ± 3E-1
0.15	4.2 ± 1E-1	5.1 ± 2E-1	4.6 ± 6E-1
0.20	6.6 ± 3E-1	5.9 ± 1E-2	6.2 ± 5E-1

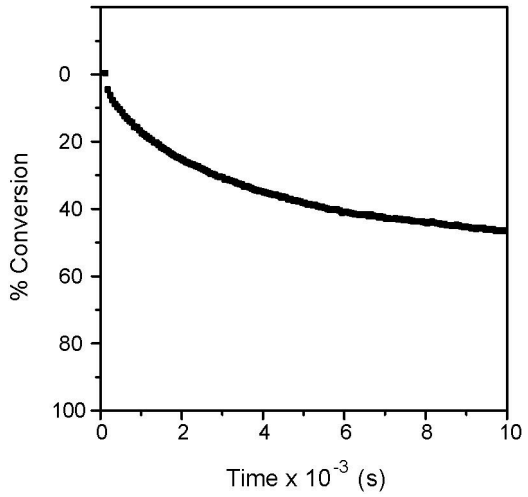

XVIII. Plot of the percent conversion for the enolization of ester **2** (0.05 M) by 1.0 equiv of LDA at -25 °C in *n*-BuOMe (11.0 equiv) and hexane cosolvent. The reaction stalls at approximately 50% conversion.

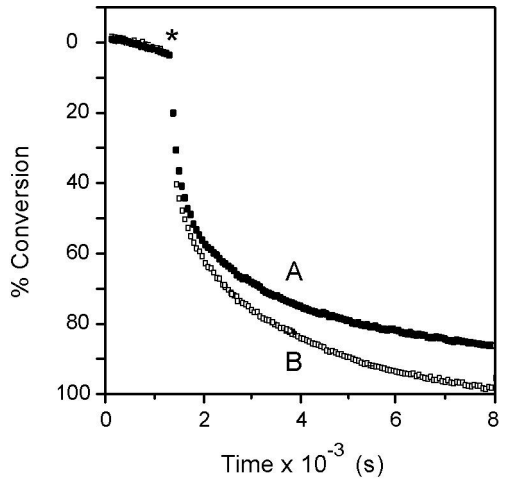

XIX. Plot of the percent conversion for the enolization of ester **2** (0.05 M) by LDA (0.1 M) at -78 °C in hexane/**C** (1.0 M) containing: (A, ■) [**B**] = 0.005 M ; (B, □) [**B**] = 0.01 M. The asterisk indicates the addition of ligand **B**.

Part 4: DFT Computational Studies

XX. Optimized geometries and free energies (*G*, Hartrees) of miscellaneous aggregates.[a,b] **A** = Me_2NLi. **E** = CH_2LiCO_2Me. **S** = Me_2O, ΔG = -154.97011. $\mathbf{A_2}$, ΔG = -284.134049. $\mathbf{A_2S_2}$, ΔG = -594.09706. $MeCO_2Me$, ΔG = -268.32786. Me_2NH, ΔG = -135.09527

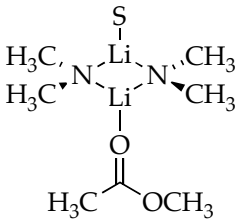

I

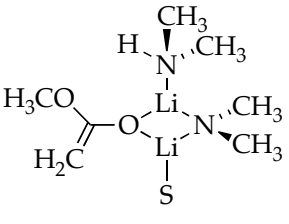

II

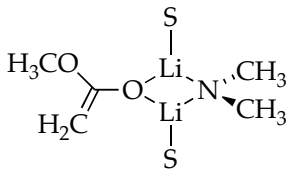

III

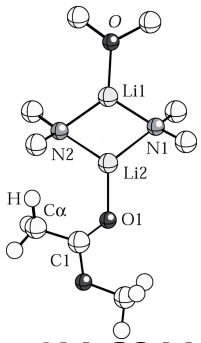

$\mathbf{A_2S}$·$MeCO_2Me$

-707.45232

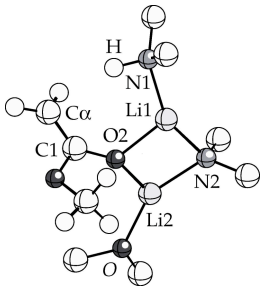

$\mathbf{AS}$·$\mathbf{E}$·Me_2NH

-707.46130

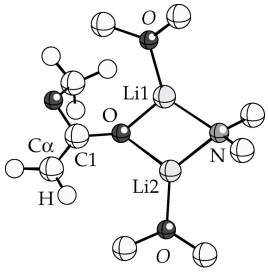

$\mathbf{AS_2}$·$\mathbf{E}$

-727.33352

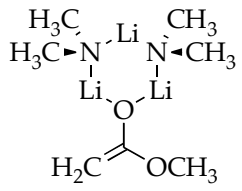

IV

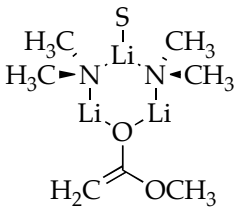

V

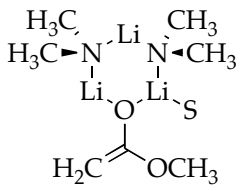

VI

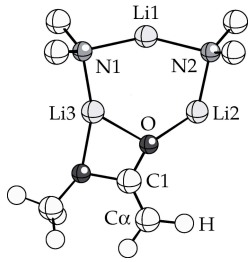

$\mathbf{A_2}$·$\mathbf{E}$

-559.47338

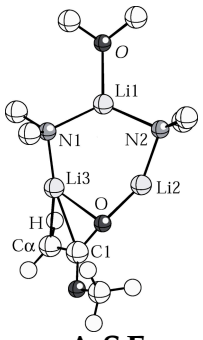

$\mathbf{A_2S}$·$\mathbf{E}$

-714.43500

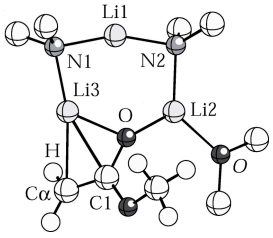

$\mathbf{A_2S}$·$\mathbf{E}$

-714.44058[d]

[a] Only selected hydrogens shown for clarity. [b] Only most stable isomers shown.

XX (*Continued*)**.**

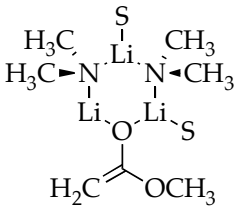

VII

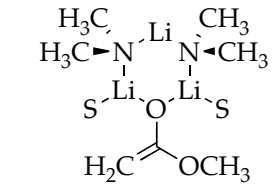

VIII

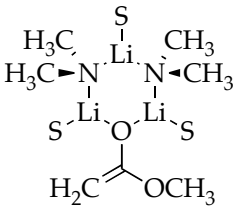

IX

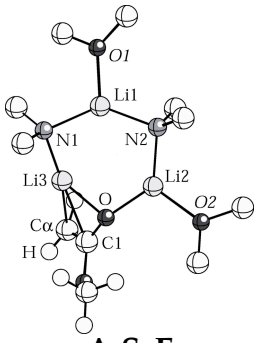

A_2S_2·E

-869.40724

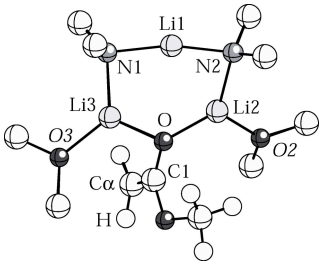

A_2S_2·E

-869.41152

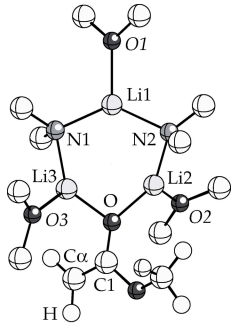

A_2S_3·E

-1024.37826

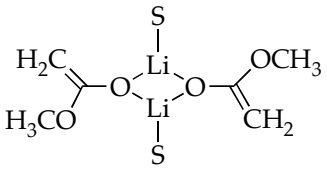

X

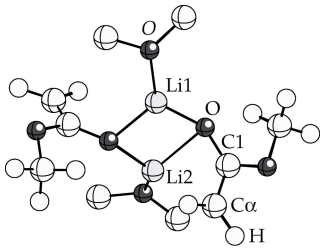

E_2S_2

-860.56997

XXI. Optimized geometries and free energies (*G*, Hartrees) of miscellaneous chelated aggregates. [a,b] **A** = Me_2NLi. **S** = $Me_2OCH_2CH_2NMe_2$ (**B**), ΔG = -328.15042. $\mathbf{A_2B_2}$, ΔG = -940.45432. $MeCO_2Me$, ΔG = -268.32786. Me_2NH, ΔG = -135.09527. $\mathbf{A_2B{\cdot}E}$, ΔG = -880.63110.

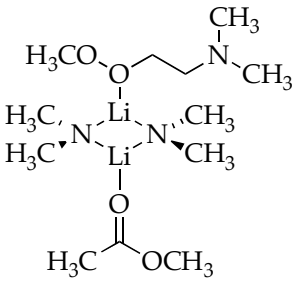

XI

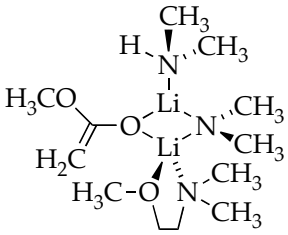

XII

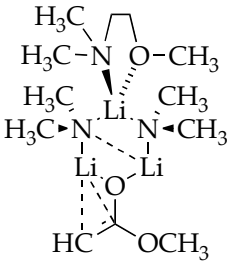

XIII

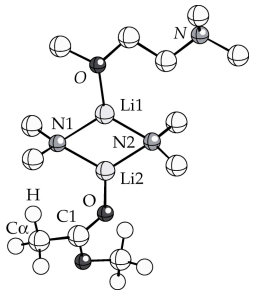

$\mathbf{A_2B{\cdot}}MeCO_2Me$
-880.63110

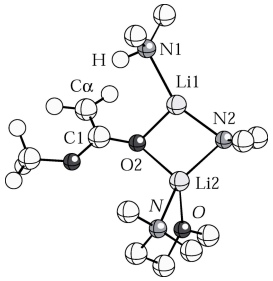

$\mathbf{AB{\cdot}E{\cdot}}Me_2NH$
-880.65218

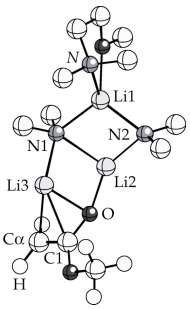

$\mathbf{A_2B{\cdot}E}$
-887.61919

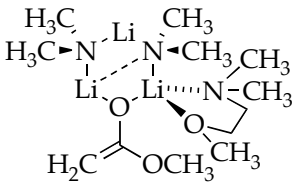

XIV

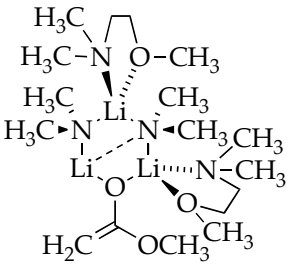

XV

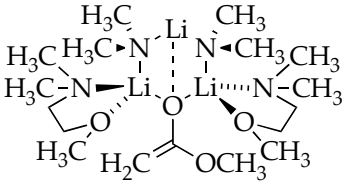

XVI

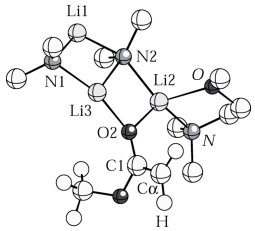

$\mathbf{A_2B{\cdot}E}$
-887.62078

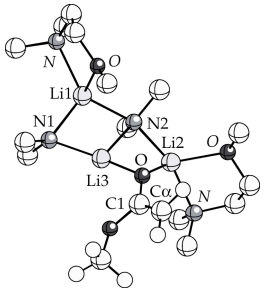

$\mathbf{A_2B_2{\cdot}E}$
-1215.78420

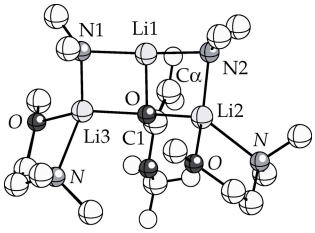

$\mathbf{A_2B_2{\cdot}E}$
-1215.78460

[a] Only selected hydrogens shown for clarity. [b] Only most stable isomers shown.

XXI (*Continued*)**.**

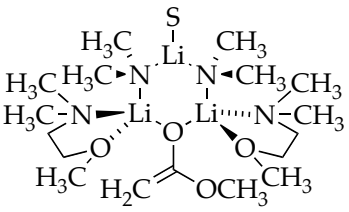

XVII

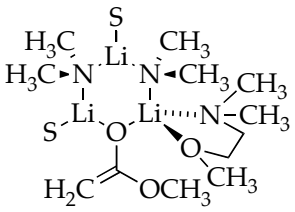

XVIII

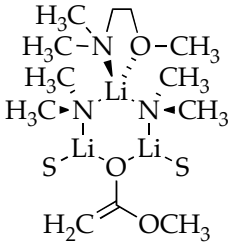

XIX

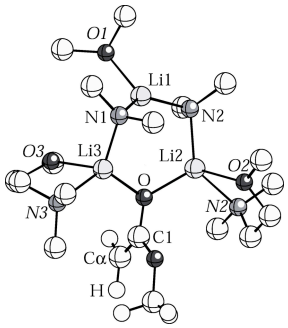

$A_2B_2S^{\cdot}E$
-1370.74270

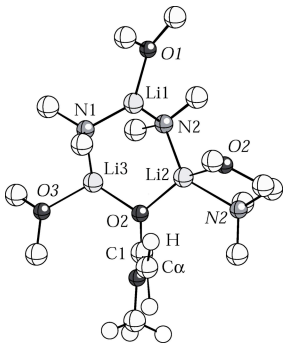

$A_2BS_2^{\cdot}E$
-1396.03023

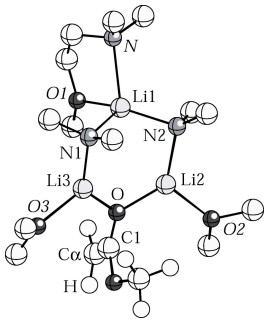

$A_2BS_2^{\cdot}E$
-1197.56116

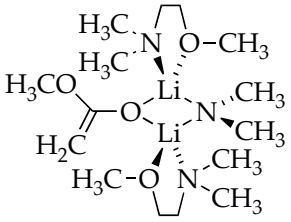

XX

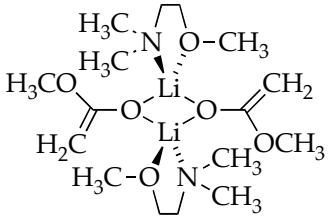

XXI

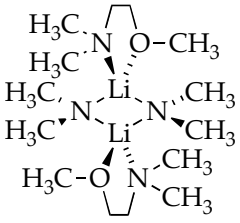

XXII

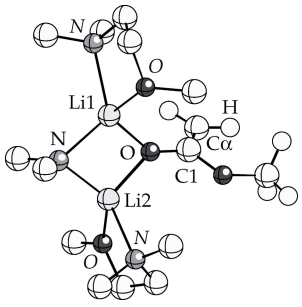

$AB_2^{\cdot}E$
-1073.70889

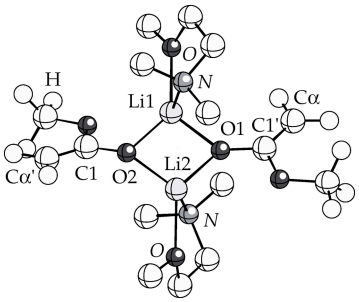

E_2B_2
-1206.95641

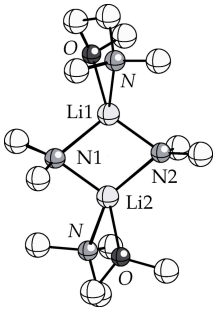

A_2B_2
-940.45148

XXII. Selected bond lengths (Å) for aggregates **I**-**XXII**.

bond	**I**	**II**	**III**	**IV**	**V**	**VI**	**VII**	**VIII**	**IX**	**X**
Li1-N1	1.99[a]	---	1.97	1.93	2.00	1.94	2.00	1.92	1.97	---
Li1-N2	1.99[a]	1.98	---	1.95	2.02	1.93	2.02	1.92	1.99	---
Li2-N2	1.99[a]	1.96	---	1.93	1.91	1.97	1.96	1.98	1.97	---
Li2-N1	1.99[a]	---	1.97	---	---	---	---	---	---	---
Li1-O	---	1.88	1.84	---	---	---	---	---	---	1.84[a]
Li2-O	---	1.84	1.85	1.77	1.76	1.84	1.84	1.87	1.86	1.96[a,d]
Li3-O	---	---	---	1.91	1.92	1.90	1.88	1.89	1.87	---
Li3-N1	---	---	---	1.95	1.93	1.93	1.92	1.98	1.98	---
Li1-*O*[b]	1.94	---	1.92	---	1.99	---	2.02	---	2.00	1.91
Li1-*N*[b]	---	2.07	---	---	---	---	---	---	---	---
Li2-*O*[b]	1.96	1.93	1.93	---	---	1.95	1.98	1.97	1.98	1.93[d]
Li2-*N*[b]	---	---	---	---	---	---	---	---	---	---
Li3-*O*[b]	---	---	---	1.98[c]	---	---	---	1.96	1.99	---
Li3-*N*[b]	---	---	---	---	---	---	---	---	---	---
Li3-C1[d]	---	---	---	---	2.23	2.24	2.25	---	---	2.27

[a]Average Li-heteroatom bond distance. [b]Italic underlined characters correspond to *O* and *N* in the ligands. [c]MeCO*O*Me-Li contact in the most stable conformation. [d]π-complexation observed.

XXII (*Continued*)**.**

bond	**XI**	**XII**	**XIII**	**XIV**	**XV**	**XVI**	**XVII**	**XVIII**	**XIX**	**XX**	**XXI**	**XXII**
Li1-N1	1.98[a]	2.07	2.18	1.89	1.98	1.96	1.98	1.97	2.04	1.99[a]	---	2.02[a]
Li1-N2	1.98[a]	1.95	1.99	1.97	2.14	1.97	1.97	1.98	2.06	---	---	2.02[a]
Li2-N2	1.98[a]	2.02	1.94	2.06	2.09	1.98	2.0	2.01	1.95	---	---	2.02[a]
Li2-N1	1.98[a]	---	2.14	---	---	---	---	---	---	1.99[a]	---	2.02[a]
Li1-O	---	1.86	---	---	---	2.06	---	---	---	1.89[a]	1.88[a]	---
Li2-O	---	1.90	1.85	1.87	1.86	1.99	1.95	1.90	1.87	1.89[a]	1.88[a]	---
Li3-O	---	1.90	1.91	1.81	1.86	1.99	1.93	1.85	1.86	---	---	---
Li3-N1	---	---	1.99	2.00	1.96	1.98	1.99	1.97	1.96	---	---	---
Li1-*O*[b]	1.97	---	2.09	---	2.09	---	2.03	2.02	2.13	2.11	2.00	2.14
Li1-*N*[b]	---	1.90	2.24	---	2.19	---	---	---	2.30	2.22	2.18	2.30
Li2-*O*[b]	1.95	2.05	---	2.06	2.06	2.13	2.18	2.11	1.99	2.06	2.04	2.14
Li2-*N*[b]	---	2.18	---	2.19	2.23	2.18	2.27	2.24	---	2.18	2.15	2.30
Li3-*O*[b]	---	---	---	---	---	2.07	2.15	2.00	2.00	---	---	---
Li3-*N*[b]	---	---	---	---	---	2.22	2.22	---	---	---	---	---
Li3-C1[c]	---	---	2.18	---	---	---	---	---	---	---	---	---

[a]Average Li-heteroatom bond distance. [b]Italic underlined characters correspond to *O* and *N* in the ligands. [c]π-complexation observed.

XXIII. Optimized geometries and free energies (*G*, Hartrees) of Me_2NLi monomer- and dimer-based enolizations.[a,b] **A** = Me_2NLi. **S** = Me_2O, ΔG = -154.97011. **B** = $Me_2OCH_2CH_2NMe_2$, ΔG = -328.15042. $MeCO_2Me$, ΔG = -268.32786. $\mathbf{A_2S_2}$, ΔG = -594.09706. $\mathbf{A_2B_2}$, ΔG = -940.45432.

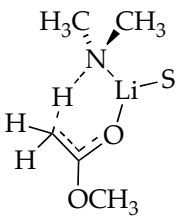

A

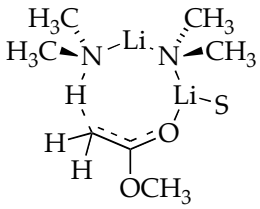

B

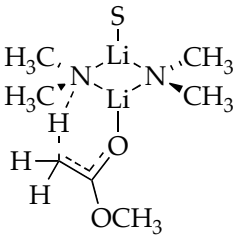

C

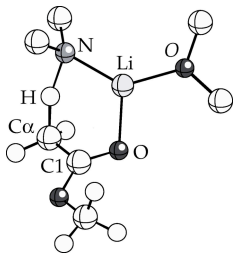

[**AS**·$MeCO_2Me$]‡
-565.35184

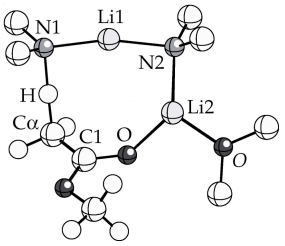

[$\mathbf{A_2S}$·$MeCO_2Me$]‡
-707.43386

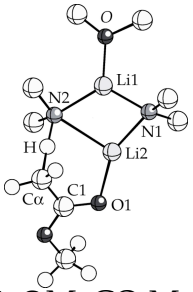

[$\mathbf{A_2S}$·$MeCO_2Me$]‡
-707.42757

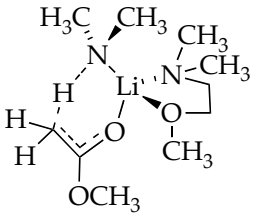

D

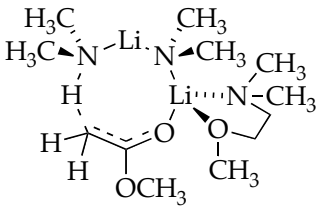

E

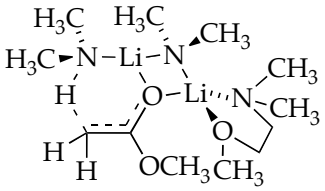

F

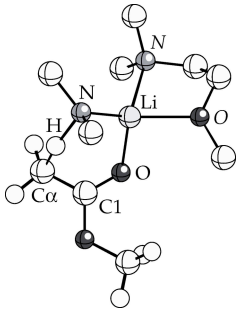

[**AB**·$MeCO_2Me$]‡
-738.53651

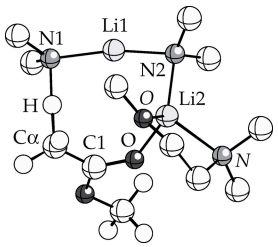

[$\mathbf{A_2B}$·$MeCO_2Me$]‡
-880.62083

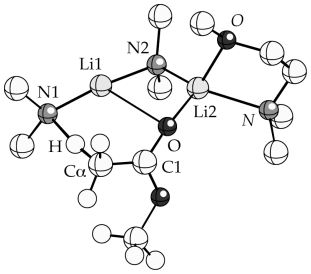

[$\mathbf{A_2B}$·$MeCO_2Me$]‡
-880.61541

[a] Only selected hydrogens shown for clarity. [b] Only most stable isomers shown.

XXIV. Optimized geometries and free energies (*G*, Hartrees) of Me_2NLi/ CH_2LiCO_2Me mixed aggregate-based enolizations.[a,b] LiB_2^+, ΔG = -663.75041.

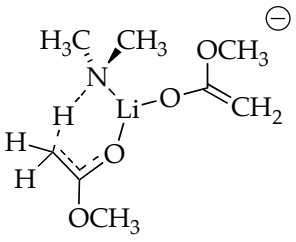

G

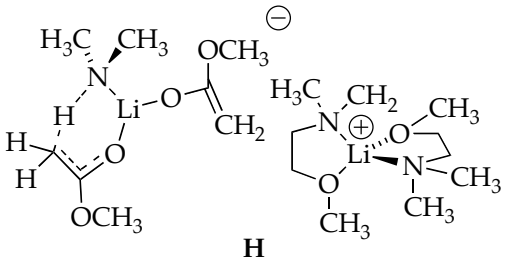

H

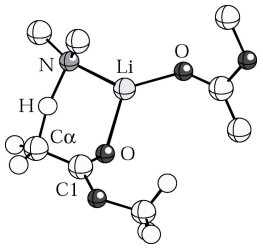

[**A**·**E**·$MeCO_2Me$]‡
-678.13849

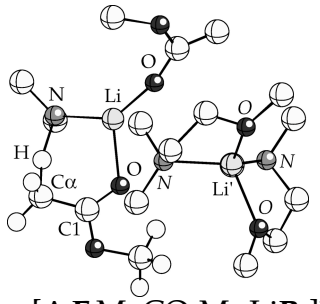

[**A**·**E**·$MeCO_2Me$·LiB_2]‡
-1341.96960

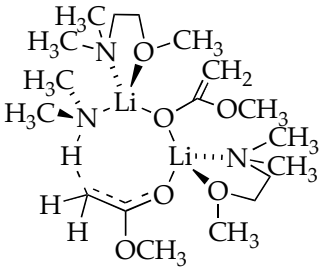

I

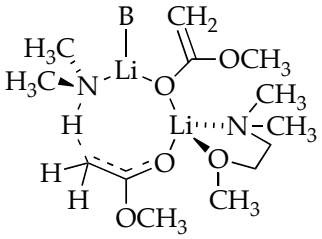

J

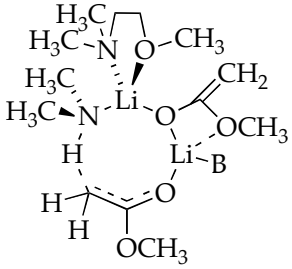

K

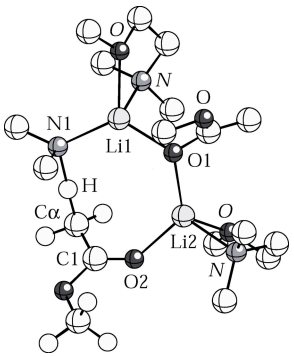

[**A**·**E**·**S**·**B**·$MeCO_2Me$]‡
-1342.01208

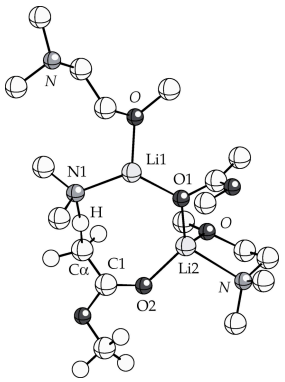

[**A**·**E**·$\mathbf{B_2}$·$MeCO_2Me$]‡
-1342.01146

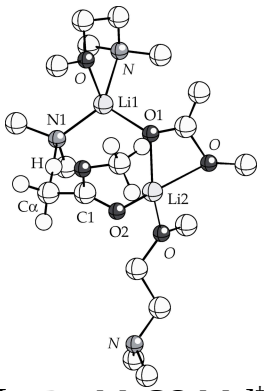

[**A**·**E**·$\mathbf{B_2}$·$MeCO_2Me$]‡
-1342.00663

[a] Only selected hydrogens shown for clarity. [b] Only most stable isomers shown.

XXV. Selected bond lengths (Å) and angles (°) for calculated transition structures **17**-**32**.[a]

bond	**17**	**18**	**19**	**20**	**28**[b]	**29**	**30**	**31**	**32**[b]
Li1-N1	1.91	2.05	1.92	1.92	---	1.96	1.99	1.97	---
Li1-N2	1.94	1.94	1.92	1.94	---	---	---	---	---
Li2-N2	1.97	1.95	2.01	1.99	1.98	---	---	---	1.99
Li2-O	1.85	1.86	1.92	1.93	1.97	1.89	1.88	1.91	2.07
C1-O	1.25	1.26	1.25	1.24	1.25	1.25	1.25	1.25	1.25
C1-Cα	1.44	1.43	1.44	1.45	1.44	1.44	1.44	1.45	1.44
Cα-H	1.30	1.41	1.33	1.24	1.30	1.31	1.28	1.27	1.30
H-N1	1.48	1.34	1.44	1.59	1.48	1.45	1.51	1.53	1.47
L1-*O*	---	1.95	---	---	---	2.01	2.09	2.08	1.79
L1-*N*	---	---	---	---	---	---	2.21	2.27	---
L2-*O*	1.95	---	2.09	2.07	2.10	2.07	1.95	2.09	2.02
L2-*N*	---	---	2.18	2.19	2.19	2.20	---	2.22	2.12
Cα-H-N1	177.2	176.5	177.0	172.9	162.4	176.1	173.8	179.1	163.4

[a]Italic underlined characters correspond to *O* and *N* in the ligands. [b]Atom numbering adapted to these transition structures.

Part 5. References

S-1. Kim, Y.-J.; Bernstein, M. P.; Galiano-Roth, A. S.; Romesberg, F. E.; Fuller, D. J.; Harrison, A. T.; Collum, D. B.; Williard, P. G. *J. Org. Chem.* **1991**, *56,* 4435.
S-2. Remenar, J. F.; Collum, D. B. *J. Am. Chem. Soc.* **1997**, *119*, 5573

(31) Gaussian 03, Revision B.04, Frisch, M. J.; Trucks, G. W.; Schlegel, H. B.; Scuseria, G. E.; Robb, M. A.; Cheeseman, J. R.; Montgomery, Jr., J. A.; Vreven, T.; Kudin, K. N.; Burant, J. C.; Millam, J. M.; Iyengar, S. S.; Tomasi, J.; Barone, V.; Mennucci, B.; Cossi, M.; Scalmani, G.; Rega, N.; Petersson, G. A.; Nakatsuji, H.; Hada, M.; Ehara, M.; Toyota, K.; Fukuda, R.; Hasegawa, J.; Ishida, M.; Nakajima, T.; Honda, Y.; Kitao, O.; Nakai, H.; Klene, M.; Li, X.; Knox, J. E.; Hratchian, H. P.; Cross, J. B.; Bakken, V.; Adamo, C.; Jaramillo, J.; Gomperts, R.; Stratmann, R. E.; Yazyev, O.; Austin, A. J.; Cammi, R.; Pomelli, C.; Ochterski, J. W.; Ayala, P. Y.; Morokuma, K.; Voth, G. A.; Salvador, P.; Dannenberg, J. J.; Zakrzewski, V. G.; Dapprich, S.; Daniels, A. D.; Strain, M. C.; Farkas, O.; Malick, D. K.; Rabuck, A. D.; Raghavachari, K.; Foresman, J. B.; Ortiz, J. V.; Cui, Q.; Baboul, A. G.; Clifford, S.; Cioslowski, J.; Stefanov, B. B.; Liu, G.; Liashenko, A.; Piskorz, P.; Komaromi, I.; Martin, R. L.; Fox, D. J.; Keith, T.; Al-Laham, M. A.; Peng, C. Y.; Nanayakkara, A.; Challacombe, M.; Gill, P. M. W.; Johnson, B.; Chen, W.; Wong, M. W.; Gonzalez, C.; and Pople, J. A.; Gaussian, Inc., Wallingford CT, 2004.
(35c) Pratt, L. M.; Newman, A.; Cyr, J. S.; Johnson, H.; Miles, B.; Lattier, A.; Austin, E.; Henderson, S.; Hershey, B.; Lin, M.; Balarnraju, Y.; Sammonds, L.; Cheramie, J.; Karnes, J.; Hyrnel, E.; Woodford, B.; Carter, C. *J. Org. Chem.* **2003**, *68*, 6387.